# Evaluation of Breast Parenchyma Changes Based on Texture Analysis in Mammography

Marta Silva Ferreira
marta.silva.ferreira@ist.utl.pt

Instituto Superior Técnico, Lisboa, Portugal

June 2017

**Abstract**

Doctors usually compare mammography images acquired at different screening times. However this is not easy. The breast is submitted to different conditions, when mammography images are acquired at distinct times. Additionally, mammographies can be different due to natural change of breast tissue. Combining the analysis of mammography texture, and observing how different texture features change over time may enhance malign breast changes, allowing an early detection of breast cancer. This work develops and validates a new tool that allows doctors to evaluate mammography images of women who underwent breast screening at sequential years. The evaluation of these mammographies is done calculating different texture features in regions of interest, and observing their evolution over time. For that pre-processing methods were first applied. Registration of mammographies was also used in order to locate in the patient mammographies acquired at different years interest regions at the same location, as well as to define regions of interest. Texture features are then calculated in these mammographies from different years. The results showed that some of these features changed before cancer was detected, however these results were not consistent in all the patients.

**Keywords:** Mammography, Breast Cancer, Time Analysis, Texture Features

## 1. Introduction

Breast cancer is the most common cancer worldwide, after lung cancer, and the most common among women, affecting about 1.4 million people every year [1]. Mammography is the standard screening method, that has been helping saving lives and improve treatment options with early detection [2], however it is not able to detect every single case, as well as it also presents a high number of false positives. It is known nowadays that there are several risk factors that may increase the probability of women developing breast cancer [3]. These include age, family history and others.

Currently, radiologists look for mammographies and other exams acquired at different times. This is not however easy, since images obtained at different screening times imply different conditions when acquired and consequently differences in the breast that may be due to normal or abnormal changes. Previous studies have attempted to detect regions of interest (ROI) by subtraction of temporal or bilateral mammographies [4][5]. To do this, mammographies need to be registered, in order to locate in the patient mammographies acquired at different years interest regions at the same location. This is also not easy, since the breast is not a rigid body. Rigid and non rigid registration methods have been developed [6].

New breast cancer risk factors, such as texture and mammography parenchyma patterns, have received some attention lately. H. Li et al. evaluated in different studies the risk of breast cancer development in women that were carriers of the BRCA1 and BRCA2 genes [7]. Texture features which included absolute grey level image intensity, first and second order statistical features, fractal analysis and power spectral analyses were extracted from regions of interest. First order statistical features are those that can be calculated from the image histogram, while second order consider spatial relationships between neighbour pixels. Fourier techniques are based on the frequency spectrum of an image or region, and fractal dimension are a measure of patterns that exhibit the same structure at different scales. The same author also investigated the effect of ROI size and location when assessing breast cancer risk. Their results showed that features selected in the central breast region behind the nipple obtained a better performance distinguishing high risk breast cancer group from low risk group.

Computing different texture features, and observing how these change over time may alert doctors for possible malignant changes.

In this work it was developed and validated a new tool that allows doctors to evaluate mammography images of women who underwent breast screening at sequential years, using different texture features and observing how these change over time. Sudden changes in these features, can reveal abnormal changes in breast parenchyma, alerting the doctor to a possible breast disease.

## 2. Methods

This work is divided into 4 different stages. These are pre-processing, images registration, definition of a region of interest and finally texture analysis. For all the stages of the study the Matlab software version R2014(b) was used.

### 2.1. Study Database

The data used in this work was provided by Hospital da Luz. Mammographies were collected from 19 female patients. Within this patient group in 13 no breast cancer was detected, in 4 breast cancer was detected, and in 2 breast cancer was never detected however the doctor suspected in sequential years the possibility of the patient having cancer. All images were obtained with a Siemens Mammomat Inspiration digital mammography system. An exception to this was observed in images acquired in 2007 and 2008, where in that case images were acquired using a Siemens Mammomat Novation digital mammography system. In addition to this, images from 2017 were also not acquired through the conventional mammography method but instead, through the reconstruction of tomossynthese images, using the prime technology of the Siemens Mammomat Inspiration mammographer. Cranio Caudal (CC) views of the left or right breast were used. All images were filtered by the Siemens Mammography system. Since different breast compression forces or positioning lead to different breast slice thickness exposed to x-rays, it was decided to exclude images whose breast slice thickness was 10 mm higher or lower than the mean value of this parameter. This was done updating the mean value each year.

### 2.2. Pre-processing

Pre-processing methods can be divided into two steps: image segmentation and normalization.

In this thesis it was necessary to detect the boundary between the breast and the background. The first step to achieve this was to transform the original image into a binary image. This was done using a threshold method, with the Matlab function *im2bw*, that converts the grey scale image into a binary image using a threshold level ranging from 0 to 1. The threshold is defined by the ratio between threshold intensity intended and the possible number of image intensity values. This resulted in a binary image with pixels corresponding to 0 staying 0, while the others are replaced by 1. In order to smooth the breast image contours, as well as remove patient specific labels, additional morphological operations that included closing and image filling, were also used. In addition to this, unnecessary image background, which occupied a significant part of the image, was also removed. In addition to image segmentation, image normalization was achieved using the histogram based method used by X. Sun et al., through shifting and stretching of the image intensity values of all the images of the same patient [8].

### 2.3. Image Registration

An hybrid registration method was first applied. This method combines a rigid global affine registration, and a non Rigid local B-Spline registration. This hybrid method allows to capture not only overall motion of the breast, but also local deformations, that since the breast is not a rigid body, cannot be explained by rigid transformations. B-spline registration uses a mesh of control points equally spaced, and B-spline functions to transform the moving image. The details of this method can be found in [9]. In addition to this, sum of square difference (SSD) was used as a similarity function and Quasi-Newton method as an optimizer [10][11]. After trying to register images using this hybrid method, it was noted that the registration resulted in a deformation of breast structures and consequently texture. Due to that, it was used a different registration method which used an affine transformation. Within this registration method an evolutionary optimizer and a mutual information (MI) based metric was used. The MI algorithm used is called Mattes algorithm. The details of this algorithm can be found in [12]. The MI metric is based on the concept that image registration can be defined as a maximization of the amount of shared information in two images or on the other hand, minimization of the amount of information in a combined image. The amount of information is measured through a metric called entropy which is defined by eq.1, where $p_A(a)$ corresponds to the probability a pixel $(x, y)$ in image $A$ has a grey-level $a$, $p_B(b)$ corresponds to the probability a pixel $(x, y)$ in image $B$ has a grey-level $b$. The MI metric can than be defined as in eq.2.

$$H(a/b) = -\sum_{a/b} p_{A/B}(a/b)\log(p_{A/B}(a/b)) \quad (1)$$

$$MI = H(a) + H(b) - H(a, b) \quad (2)$$

For the MI metric 2 parameters needed to be defined. The first one is the number of pixel samples

$J$ used. In case it was opted not to sample all the pixels, the algorithm randomly chooses a set of samples from the image, and so the registration results might not be the same every time the code is compiled. Due to that, it was decided to use all the pixels. The second parameter corresponds to the number of histogram bins $N$ used.

Table 1: Mutual Information Similarity metric parameters

| parameter | $J$ | $N$ |
|---|---|---|
| value | All Pixels | 100 |

In regards to the Evolution Optimizer, this optimization approach is based on the Evolution strategy approach [13].Once again, within this optimization method 4 different parameters were chosen. These were the Grow factor $c_{grow}$, the initial search Radius $d_0$ and $\epsilon$, which corresponded to the minimum size of the search radius and finally, the maximum number of iterations $k$. The final chosen parameters can be seen in tables 1 and 2.

Table 2: Evolution Optimizer parameters

| parameter | $c_{grow}$ | $\epsilon$ |
|---|---|---|
| value | 1.05 | $1.5 \times 10^{-6}$ |
| parameter | $d_0$ | max $k$ |
| value | $6.25 \times 10^{-3}$ | 500 |

An empiric choice of these values was done trying a different set of parameters and visually observing which ones resulted in a better alignment of the breast contours of the two mammographies. For $k$ and $N$ parameter Pearson correlation was also used to help assess the quality of registration and choose the best parameters. For registering both images, a fixed image was defined for each patient. This image was chosen to be the oldest of the images acquired between 2009 and 2017. After registration with the defined parameters, it was also measured the quality of each registration using Pearson correlation.

### 2.4. Region of interest

An image visualization tool was developed in order to detect suspicious regions. Regions of interest were selected in one mammography and automatically observed in the remaining mammographies from the sequential years. Texture features were then calculated in those ROI(s), and their change along the years analysed. This was done through different steps:

- **Define interest regions** - Interest regions were defined, through the subtraction pixel by pixel of each registered image from the fixed image, and from the image from the previous year. Two thresholds corresponding to these differences could then be manipulated, in order to select regions according to a bigger or lower difference. In addition to this, skin was removed through 4 sequential erosion operations with a square structuring element with 20 pixels of width, and was not included in the subtraction.

- **Automatic region selection** - Automatic region selection was done implementing the More Neighbourhood algorithm for tracing the boundaries of a binary image.

- **Remove lower risk regions** - In order to remove suspicious regions that could be due to wrong registration or due to normal differences of breast parenchyma, some regions were excluded. Two methods were first implemented to do this. Since even after removing skin some of the suspicious regions were found near the breast-background boundary, it was calculated the Euclidean distance for all the boundary points in each suspicious region, and removed regions whose minimum distance to the breast-background boundary was less than 50 pixels. Eccentricity was also calculated to remove elongated regions appearing near the breast background border.

### 2.5. Texture Analysis

After detecting suspicious regions, it was intended to investigate how texture of these regions changed through the years. Texture analysis was done defining rectangular regions with different sizes around these ROI(s). In addition to this, regions situated around the nipple retroaerolar region were also analysed due to the big importance given in this areas in literature [14]. In order to evaluate the change of texture in these ROI(s), texture features were also computed in the entire breast, so that the local ROI(s) could be compared to the overall change of breast texture. Texture features calculated included: first and second order statistical features, absolute grey level values of the image, run length features, fractal dimension and local binary patterns.

- **First and Second Order Statistical Features**-First order statistical features, correspond to individual pixel properties, that are not spatially dependent and can be computed from the image histogram. Four first order statistical features were calculated from the image grey-level intensity histogram. These were: average grey level, variance, skewness and kurtosis. In addition to first order features, second order statistical features consider the interactions between neighbour pixels, and are extracted from the grey-level co-occurrence Matrix (GLCM). These matrix entries represent the probability of finding a pair of pixels within the image. 12 texture features were extracted from this matrix as done in [15]. These features included: energy, entropy, Contrast, Correlation, inverse difference moment, Sum of Squares, sum average, sum variance, sum entropy, difference variance, difference entropy and information measure of correlation. Two additional features called cluster shade and dissimilarity were also computed as done in [16]. The region selected was quantized into 256 grey-level values for constructing the GLCM and used a distance of 1 pixel, with 4 different angles: 0, 45, 90 and 135 degrees.

- **Absolute Grey-level values-** It was calculated the maximum and minimum Grey-level intensity. Additionally it was also computed the grey level intensity , where 95 (TH95) and 5 (TH5)% of the histogram bins of the image histogram were located.

- **Run length Features-** Grey level Run length features were measured through Grey level run length matrices. These matrices provide the number of times a certain grey value appears in the image consecutively within a certain direction. Five features from the Run length matrix were computed as done in [17]. These were short run emphasis, long run emphasis, Grey level Nonuniformity, run percentage and run length Nonuniformity. Regions selected were quantized into 256 grey levels and the run length matrix constructed using 4 different angles: 0, 45, 90 and 135 degrees.

- **Fractal dimension-** Fractal dimension, as the name says, is a measure of self-similar patterns, more precisely, repeating patterns that exhibit the same structure at different scales. Fractal dimension was computed through a method called box counting method. In this method several boxes are determined at each pixel. Each box surface has the dimensions of the pixel size and height corresponding to the brightness of that pixel in the image. In order to measure the fractal dimension the surface area of this boxes needs to be determined [18]. Using eq.3 the fractal dimension ($D$) can be estimated, where $\epsilon$ corresponds to the pixel size and $A$ to the surface area [18].

$$D = 2 - \frac{\Delta \log_e[A(\epsilon)]}{\Delta \log_e[\epsilon]} \tag{3}$$

- **Local Binary Pattern-** Local Binary Patterns (LBP), which are texture operators that characterize each pixel neighbourhood by comparing each pixel intensity with its neighbours and defining each pattern as an unique binary number. The number of neighbourhood pixels to be considered, as well as the radius distance from the neighbourhood points to the centre pixel determines different local binary patterns. Rotational Invariant local binary patterns were calculated as done in [19]. For this thesis it was opted to use 8 neighbours and a radius of 1 for measuring LBP. To evaluate the difference between these patterns on the different mammographies from the different years, it was computed the histogram of each local binary pattern image. The absolute value of the difference of these vectors, was then taken to measure the difference between the different patterns.

## 3. Results

In this section, the most important results are presented.

### 3.1. Pre-processing

In the first pre-processing step the breast boundary was detected and some of the unnecessary image background removed. In addition to this, the images were normalized. In figure 3.1, it can be see an example of a pre-processed image, with labels and some background removed, and already normalized.

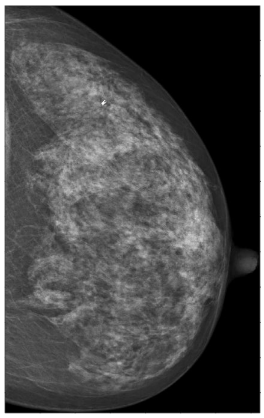

Figure 1: Mammography pre-processing.

The breast-background boundary was detected successfully in all the images. However, in some of them due to breast wrong positioning dark regions closer to the breast Pectoralis Muscle could be seen and were also detected as being part of the breast region.

### 3.2. Image Registration

The next step was image registration. As explained in section 2.3, it was applied two different registration methods: an hybrid registration using an Affine and a non-rigid B-spline transformation, and additionally another method using a unique rigid affine transformation. An example of a registered image using both methods and their superposition with the original image can be seen in figure 2 and 3, respectively.

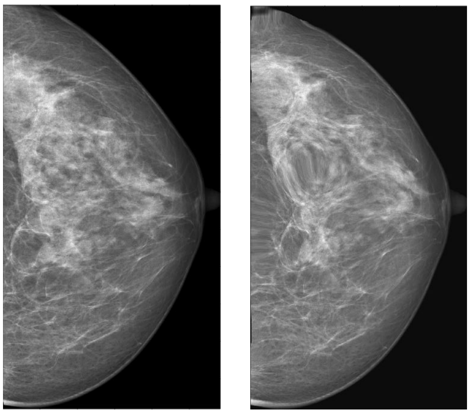

(a) (b)

Figure 2: Image registration.
(a) Moving image registered using an Affine Transformation. (b) Moving image registered using an hybrid Transformation.

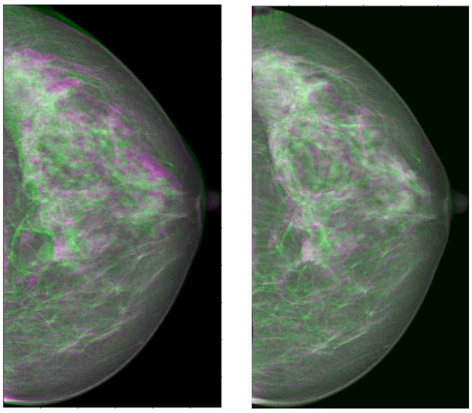

(a) (b)

Figure 3: Superposition of the moving image and fixed image.
(a) Affine Transformation; (b) Hybrid Transformation.

As it can be seen from these figures, the non Rigid method resulted in a non realistic deformation of the breast and so it was decided that the most appropriate method to be used was the affine transformation. After defining what method to use, it was needed to choose which Affine transformation parameter values, namely parameters from the Mutual information similarity metric and the Evolution Optimizer, were the most appropriate for optimizing this transformation. It was tried several parameters for each of the 4 parameters of the optimizer, and for the 2 parameters of the mutual information metric. Maximum number of iterations and number of histogram bins used were the variables which had shown greater influence in image registration. The choice of the remaining variables was set to the default Matlab values. To more easily chose the right parameter $k$ and $N$, in addition to visually observing the alignment between the two images breast contours, it was also calculated the Pearson correlation between all the images of 4 selected patients, and the corresponding chosen images used as fixed in the registration step. Five different $k$ values were tested (100, 300, 500, 700 and 900). In some of the images changing the parameter k did not affect the quality of the registration. On the other hand, in other images the variation of the $k$ value had a greater influence. The choice of $k$ was based in those images, where a bigger variation of the Pearson correlation coefficient for different $k$ values was noted. The same was done for choosing the optimizer parameter $N$. In that case, 4 different values for $N$ were tried (50, 100, 250 and 500).

Breast registration is not easy, since as already referred, breast is not a rigid body. Different forces applied when compressed can lead to deviations of breast structures. Due to that, errors in breast registration occurred. Deviation of breast nipple position or breast contour from the fixed image were sometimes observed.

### 3.3. Image Visualization Tool

In order to select a region of interest in all the sequential years' patient mammographies, an image visualization tool was developed. As described in section 2.4, this application permits an easy observation and comparison of the images, automatic selection of a ROI, which is detected through the differences between prior and current mammographies. Finally, it also allows to measure different texture features in these regions from all the images. This tool, was a result of a suggestion made by doctor Pedro Macedo, who followed this study, since currently it does not exist a similar software. A preview of this tool applied to one of the patients can be seen in figure 4.

In this figure 3 different images can be seen. The first two images, counting from the most left one, correspond to two pre-processed images, from sequential years. The corresponding years of these two images can be seen at the left part of the image. The third and most right image corresponds to the most recent image of those two, and already registered to the fixed defined image. The application opens all the patient images, in pairs of sequential years in different figures, each one with these three images. Figure 4 shows one of these figures. In

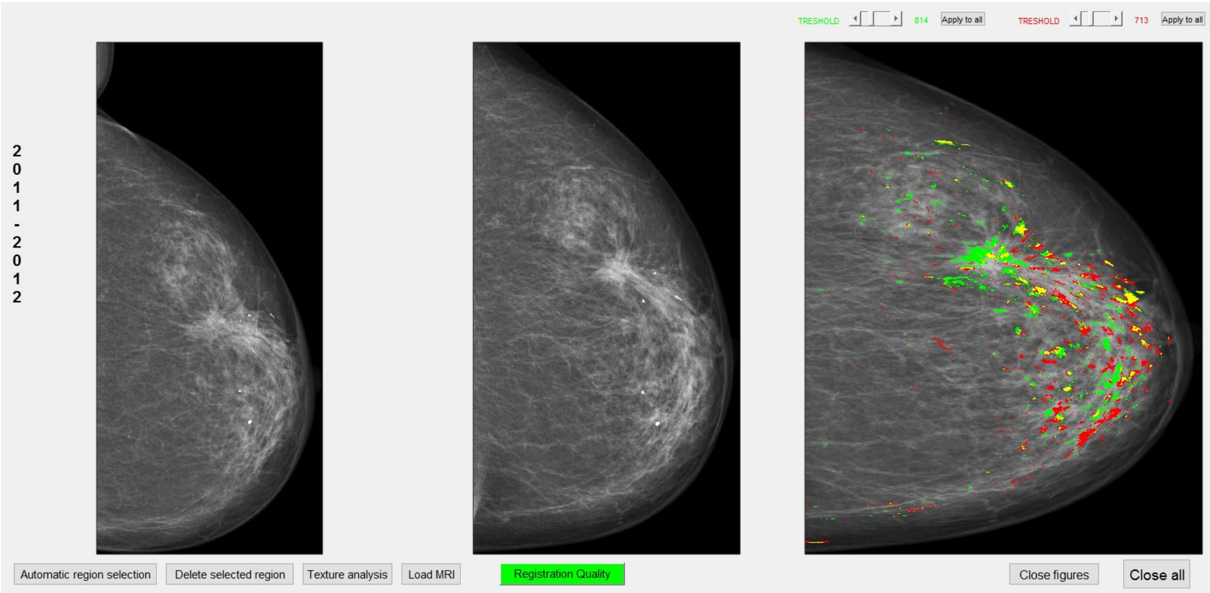


Figure 4: Image visualization tool.

the third image can also be seen green, red and yellow spots. These spots correspond to the calculated subtraction between the two images, represented in a colour scale and superimposed to the registered image. The green spots correspond to the difference between the current image and the image from the previous year. The red spots refer to the difference between the current image and the image chosen as fixed image in the registration step (image where all the other images were registered to). Finally, the yellow spots correspond to spots where both of these described differences overlap. These differences are controlled by two thresholds, located in the upright part of the image. The application also allows to apply the same threshold to all the registered images of the different figures.

Due to the fact that in most of the patients too many regions were marked, this method of selection of a region of interest did not show to be very reliable. Due to that, when choosing a ROI for texture analysis it was decided to not only select regions marked with green or red spots, but also to select regions in the nipple retroaerolar region of the breast, due to their importance given in literature when assessing the risk of breast cancer development, as refereed in section 1.

Additional buttons with different functionalities can be seen in figure 4. At the bottom left of the figure there are 4 different buttons. The first one, **Automatic Region Selection**, automatically defines contours around the red or green spots according to the choice of the operator. In addition to this, within this region also removes lower risk regions, probably detected due to a bad registration between images and most of the times detected near the skin region. In addition to this, the **Delete Selected Region button** allows the user to delete unwanted selected regions. The third and most important functionality is **Texture Analysis**. After clicking on this button he/she should select which texture features wants to measure from the list of features explained in section 2.5. A square region is chosen with the computer mouse in one of the images, and selected automatically at the same coordinates in the remaining registered images, where the texture features are calculated (figure 3.3). Texture analysis of selected regions of mammographies from the used database was done in this study. These results can be seen in the section 3.4.

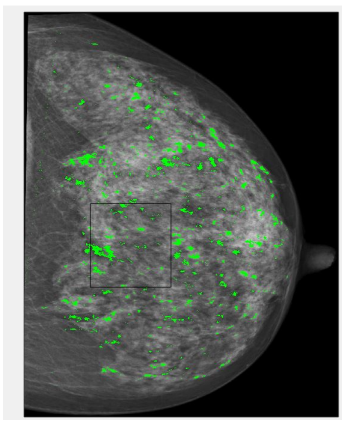

Figure 5: Square region selected for texture analysis.

The fourth button **Load MRI** adds patients magnetic resonance images (MRI) if these exist, allowing the user to visualize this set of images indicated by the image slice at the upper part of the MRI image, and in addition to this, to visualize the older mammography image (at the centre), and most recent registered one (at the right part). The last button **Registration Quality** alerts the user to possible bad registration. The button is shown in three possible colours according to the quality of registration: green (good registration), yellow (average registration) and red (bad registration). Each image registration was considered to be good if the correlation coefficient was higher than 0.9, average if between 0.8 and 0.9 and bad if lower than 0.8. Clicking on this button also allows the user to see the correlation coefficient calculated to assess registration quality.

### 3.4. Texture Analysis

Texture analysis was done observing how the different texture features change over time. In order to do this, square regions selected in the registered mammographies were used. Features were also measured in the entire breast region. The analysis of the variation of these features along the years in the selected regions was compared with those measured in the entire breast region. Texture analysis was done in three different groups of patients. In this section some of the results of 3 selected patients from the study database are shown. Three groups of patients were selected with these 3 patients: 1 where breast cancer was detected (patient 4), 1 patient where breast cancer was never detected but where the doctor suspected in sequential years the possibility of the patient having cancer (patient 13), and finally 1 patient where breast cancer was not detected (patient 16). In the plots where second order statistical features are presented, only features measured through GLCM using 0 degrees are shown. In addition to this, images from 2007 and 2008, as well as images from 2017, are marked in the plots with a red *.

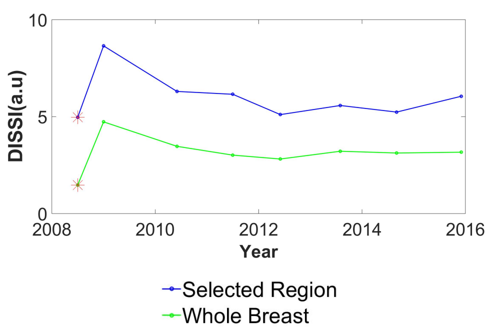


Figure 6: Dissimilarity variation through the years in patient 4. Region selected in the location of the tumour.

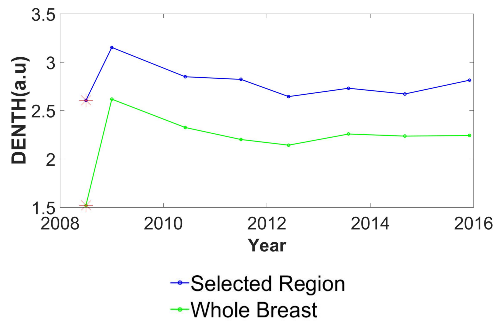


Figure 7: Difference Entropy variation through the years in patient 4. Region selected in the location of the tumour.

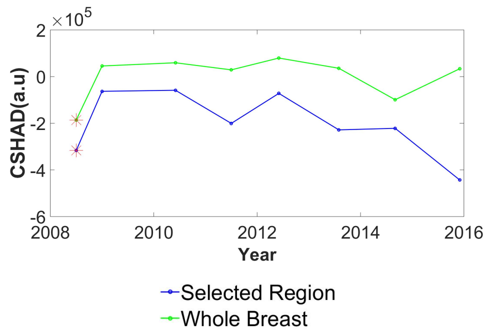


Figure 8: Cluster Shade variation through the years in patient 4. Region selected in the location of the tumour.

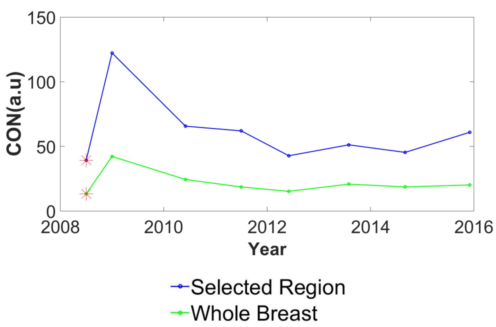


Figure 9: Contrast variation through the years in patient 4. Region selected in the location of the tumour.

## 4. Discussion

Comparing and analysing the overall results obtained, some aspects should be enhanced. The first one is that big discrepancies between features priorly to 2009 and after 2017 were observed, as a result of the different texture caused by different equipment or method used in mammography image acquisition. Second, there was observed some correlation between features. Difference entropy and dissimilarity were correlated in all the presented patients, except in patient 16. Moreover, it was

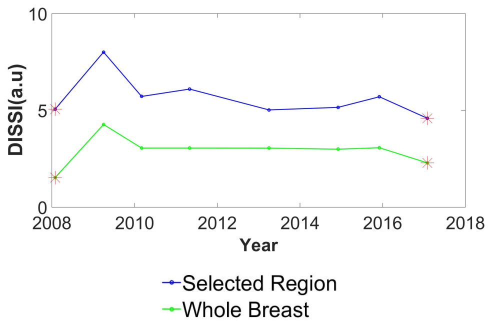


Figure 10: Dissimilarity variation through the years in patient 13. Region selected in the retroaerolar region of the breast. Suspected cancer patient.

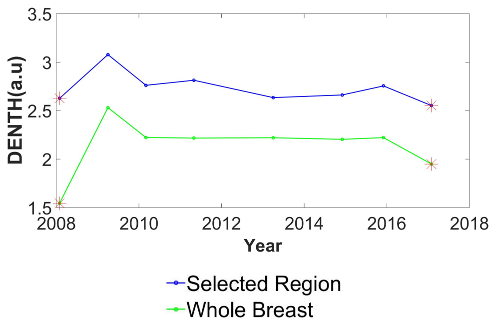


Figure 11: Difference Entropy variation through the years in patient 13. Region selected in the retroaerolar region of the breast. Suspected cancer patient.

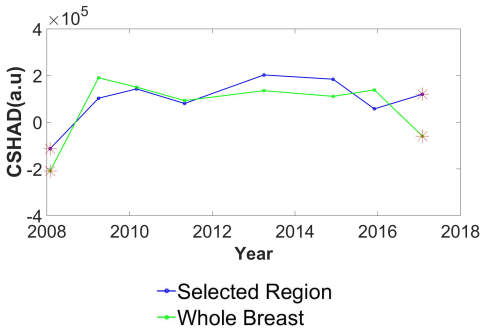


Figure 12: Cluster Shade variation through the years in patient 13. Region selected in the retroaerolar region of the breast. Suspected cancer patient.

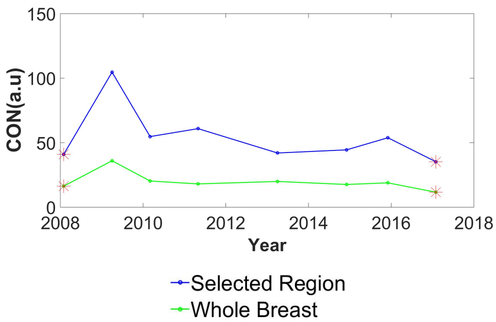


Figure 13: Contrast variation through the years in patient 13. Region selected in the retroaerolar region of the breast. Suspected cancer patient.

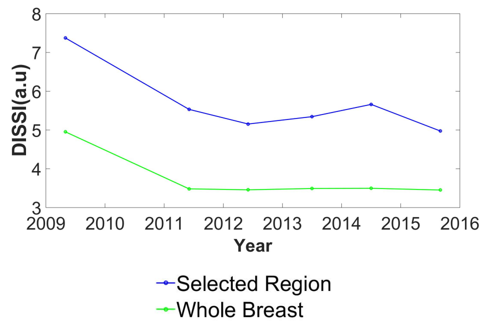


Figure 14: Dissimilarity variation through the years in patient 16. Region selected in the retroaerolar part of the breast. No cancer was detected in this patient.

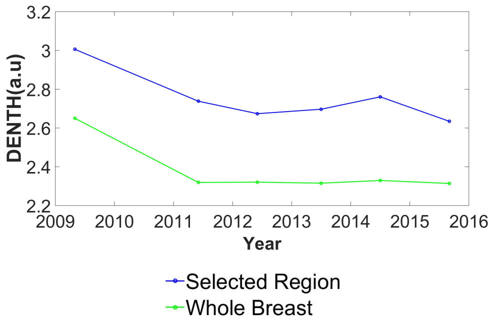


Figure 15: Difference Entropy variation through the years in patient 16. Region selected in the retroaerolar part of the breast. No cancer was detected in this patient.

observed that some of the features demonstrated differences in their variation along the years comparing with the ones observed in the entire breast such as in Cluster shade, Difference Entropy, dissimilarity and contrast. This change was not consistent in the different patients, meaning that, in some cases there was a decrease in these features while in other cases there was an increase. In addition to this, in some of the patients changes of these features were also observed in previous years, and not only in years closer to date where breast cancer was detected. Furthermore, the modification of the value of the presented features along the years may depend on several factors that are not being taken into consideration. For instance, their change can depend on the type of tumour, which is not being considered in this study. In spite of these features having proved to be good when assessing

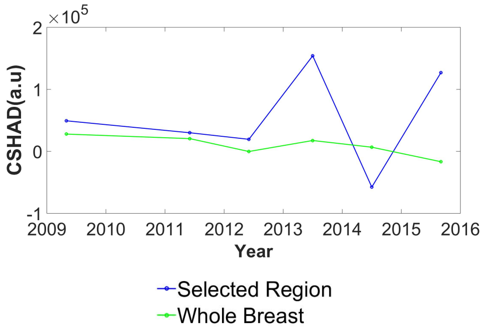


Figure 16: Cluster Shade variation through the years in patient 16. Region selected in the retroaerolar part of the breast. No cancer was detected in this patient.

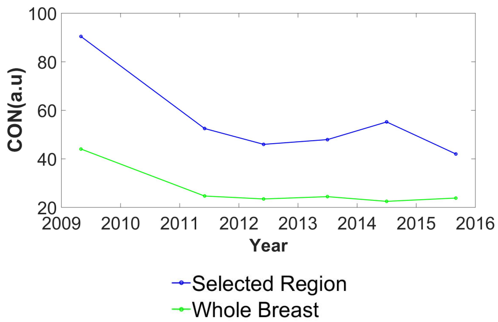


Figure 17: Contrast variation through the years in patient 16. Region selected in the retroaerolar part of the breast. No cancer was detected in this patient.

breast cancer risk, as described in section 1, there are not many studies that evaluate these features using mammographies taken at different years. Additionally, there was not found any study that uses the difference of texture features calculated in current and prior mammography to detect cancer.

## 5. Conclusions

This thesis presents a new software tool that allows mammography analysis over time, by registering mammographies acquired in different years, and pointing areas with larger anatomic changes. Additionally, it also presents a preliminary study of texture analysis in these regions. This texture analysis is done observing how this texture features change over time.

To do this, this work is divided into several steps. The first steps correspond to pre processing and normalization. The second stage is image registration. Registration allows an automatic selection of a ROI, at the same location in all the patients' mammographies, as well as selecting regions of interest, by subtracting registered images acquired in sequential years. This was done implementing a mammography image visualisation tool, which allows to observe Mammographies along the years as well as to measure different texture features in all the mammographies of the patient from different years. In order to eliminate ROI(s) that were due to natural breast changes or bad registration it was also implemented a method, which eliminates these regions. They were eliminated taking into consideration their shape and position. Finally, different texture features are evaluated in these selected regions.

From the results it was observed, when comparing the entire breast region with some of the selected regions, a different behaviour of some of the features in years before cancer being detected. These features were Cluster shade, difference entropy, dissimilarity and contrast. Due to the size of our database, which was small and only contained a few patients in whom breast cancer was detected, it was not possible to prove the robustness of this method. Additionally, some variance in these features was also observed in patients where no breast cancer was detected.

This work presents a preliminary study and due to that a lot of work can be done to improve its different steps. To start, a proper database of women who had sequential mammographies needs to be constructed. In this database patients where breast cancer was detected should also be divided according to the type of tumour that had been diagnosed. Additionally, a better optimization of the registration parameters and/or selection of other registration methods, as well as investigation of metrics that can be used to reduce the big number of regions selected, can also be studied. New texture features can also be explored, as well as the combination of current features with other factors associated with breast cancer risk. Finally, deep learning algorithms can also be used to classify the change of mammography texture patterns as cancer or not.

## References


[1] J Ferlay, I I Soerjomataram, R Dikshit, S Eser, C Mathers, M Rebelo, D M Parkin, D Forman, and F Bray. Cancer incidence and mortality worldwide : sources , methods and major patterns in GLOBOCAN 2012. *International Journal of Cancer*, 136(5):359–386, 2012.

[2] American cancer Society. Cancer Facts & Figures 2016. Technical report, American Cancer Society, Atlanta, 2016.

[3] S Eva Singletary. Rating the Risk Factors for Breast Cancer. *Annals of Surgery*, 237(4):474–482, 2003.

[4] Arturo J. Méndez, Pablo G. Tahoces, María J. Lado, Miguel Souto and Juan J. Vidal.

Computer-aided diagnosis : Automatic detection of malignant masses in digitized mammograms. *Medical Physics*, 25(6):957–964, 1998.

[5] Fangfang Yin, Maryellen L Giger, Kunio Doi, Charles E Metz, Carl J Vyborny, and Robert A Schmidt. Computerized detection of masses in digital mammograms : Analysis of bilateral subtraction images. *Medical Physics*, 18(955):955–963, 1991.

[6] Saskia Van Engeland, Peter Snoeren, Jan Hendriks, and Nico Karssemeijer. A Comparison of Methods for Mammogram Registration. *IEEE Transactions on Medical Imaging*, 22(11):1436–1444, 2003.

[7] Gretchen L Gierach, Hui Li, Jennifer T Loud, Mark H Greene, Catherine K Chow, Li Lan, Sheila A Prindiville, Jennifer Engwong, Peter W Soballe, Claudia Giambartolomei, Phuong L Mai, Claudia E Galbo, Kathryn Nichols, Kathleen A Calzone, Olufunmilayo I Olopade, Mitchell H Gail, and Maryellen L Giger. Relationships between computer-extracted mammographic texture pattern features and BRCA1 / 2 mutation status : a cross-sectional study. *Breast Cancer Research*, 16(4), 2014.

[8] Xiaofei Sun, Lin Shi, Yishan Luo, Wei Yang, Hongpeng Li, Peipeng Liang, Kuncheng Li, Vincent C T Mok, Winnie C W Chu, and Defeng Wang. Histogram-based normalization technique on human brain magnetic resonance images from different acquisitions. *BioMedical Engineering OnLine*, 14(73):1–17, 2015.

[9] D Rueckert, L I Sonoda, C Hayes, D L G Hill, M O Leach, and D J Hawkes. Nonrigid Registration Using Free-Form Deformations : Application to Breast MR Images. *IEEE Transactions on Medical Imaging*, 18(8):712–721, 1999.

[10] Arnau Oliver, Xavier Llad, Jordi Freixenet, Joan Mart, Joan Carles Vilanova, and Robert Mart. Revisiting Intensity-Based Image Registration Applied to Mammography. *IEEE Transactions on Information Technology in Biomedicine*, 15(5):716–725, 2011.

[11] Stefan Klein, Marius Staring, and Josien P W Pluim. Evaluation of Optimization Methods for Nonrigid Medical Image Registration Using Mutual Information and B-Splines. *IEEE Transactions on Image Processing*, 16(12):2879–2890, 2007.

[12] Smriti Raghunathan, Don Stredney, P Schmalbrock, and Bradley D Clymer. Image Registration Using Rigid Registration and Maximization of Mutual Information. In *Annual Medicine Meets Virtual Reality Conference*, Long Beach, CA., 2005.

[13] Martin Styner, Christian Brechb, and Guido Gerig. Parametric estimate of intensity inhomogeneities applied to MRI. *IEEE Transactions on Medical Imaging*, 19(3):153–165, 2000.

[14] Hui Li, Maryellen L Giger, Zhimin Huo, Olufunmilayo I Olopade, Li Lan, Barbara L Weber, Ioana Bonta, Hui Li, Maryellen L Giger, Zhimin Huo, and Barbara L Weber. Computerized analysis of mammographic parenchymal patterns for assessing breast cancer risk : Effect of ROI size and location Computerized analysis of mammographic parenchymal patterns for assessing breast cancer risk : Effect of ROI size and location. *Medical Physics*, 31(3):549–555, 2004.

[15] K.Shanmugam Robert M. Haralick and Its'hak Dinstein. Textural Features for image classification. *IEEE Transactions on Systems, man and Cybernetics*, 3(6):610–621, 1973.

[16] Leen-kiat Soh, Leen-kiat Soh, Costas Tsatsoulis, and Senior Member. Texture Analysis of SAR Sea Ice Imagery Using Gray Level Co-Occurrence Matrices Texture Analysis of SAR Sea Ice Imagery Using Gray Level Co-Occurrence Matrices. 1999.

[17] Mary M. Galloway. Texture Analysis Using Gray Level Run Lengths. *Computer Graphics and Image Processing*, 4(2):172–179, 1975.

[18] Rangaraj M. Rangayyan. *Biomedical Image Analysis*. CRC Press, Calgary, Alberta, 2005.

[19] Timo Ojala, Matti Pietikäinen, and Topi Mäenpää. Multiresolution Gray Scale and Rotation Invariant Texture Classification with Local Binary Patterns. *IEEE Transactions on Pattern Analysis and Machine Intelligence*, 24:971–987, 2002.